IEEE Access
Multidisciplinary | Rapid Review | Open Access Journal

Received January 8, 2020, accepted January 30, 2020, date of publication February 10, 2020, date of current version February 25, 2020.

Digital Object Identifier 10.1109/ACCESS.2020.2972916

The Progress of the Helicopter-Borne Transient Electromagnetic Method and Technology in China

XIN WU, GUOQIANG XUE, AND YIMING HE

Key Laboratory of Mineral Resources, Institute of Geology and Geophysics, Chinese Academy of Sciences, Beijing 100029, China
College of Earth and Planetary Sciences, University of Chinese Academy of Sciences, Beijing 100049, China
Innovation Academy for Earth Science, Chinese Academy of Sciences, Beijing 100029, China

Corresponding author: Guoqiang Xue (ppxueguoqiang@163.com)

This work was supported in part by the Scientific Equipment Instrument and Development Project of Chinese Academy of Sciences under Grant YJKYYQ20190004, in part by the China Postdoctoral Science Foundation under Grant 2019M660043, in part by the Research and Development of Key Instruments and Technologies for Deep Resources Prospecting under Grant ZDYZ2012-1-03, in part by the Key Technologies for Deep Resources Prospecting of Beijing Municipal Science and Technology Commission under Grant Z181100005718001, and in part by the Natural Science Foundation of China (NSFC) under Grant 41830101.

ABSTRACT The central and western regions of China have appropriate conditions for mining development, but there are many deserts, swamps and forest-covered areas in this vast land. As a result, the traditional on-ground methods are difficult to carry out efficiently in these areas. The airborne transient electromagnetic method can implement detection over large areas rapidly and efficiently, and play an important role in terms of resource and environment detection. In recent years, two Helicopter-borne Transient electromagnetic (HTEM) systems, CHTEM-I and CAS-HTEM, were developed in China. In this paper, the difficult issues in the development of HTEM hardware and software will be analyzed, firstly. By tracing the specific technical paths to solve these difficult issues, the latest research achievements in the development process of CHTEM-I and CAS-HTEM will be expounded. Finally, we would like to briefly discuss the research and development direction of HTEM technology in China to promote further development of the research and application of this technology.

INDEX TERMS Helicopter, transient electromagnetic, system design, data processing, exploration.

I. INTRODUCTION

The Airborne Transient Electromagnetic (ATEM) Method is a geophysical electromagnetic prospecting method, whose devices are mounted on a flight platform. As shown in Fig.1, the primary field is transmitted toward the earth using a transmitter loop suspended on the flight platform, and excites the eddy current in the earth's interior. The decay of the eddy current excites a new electromagnetic filed (secondary field), and the subsurface structure will be detected by observing the secondary field [1]. An ATEM system mainly includes the transmitter, receiver, sensor and platform. Because of the flight measurement, the ATEM can effectively overcome the constraints of the terrain and geomorphological conditions, and efficiently and accurately obtain the information of the subsurface structure. The ATEM method has been widely applied in the exploration of mineral, groundwater and other resources [2]–[5].

The associate editor coordinating the review of this manuscript and approving it for publication was Su Yan.

In accordance with the selected platform, the ATEM can be further divided into two types: fixed-wing aircraft-borne Transient Electromagnetic (FTEM) and Helicopter-borne Transient Electromagnetic (HTEM). Due to the strong load capacity and large power supply, the fixed-wing aircraft gradually became the main choice of the ATEM system platform in the 1970s, and this situation lasted until about 2000. Since then, with the change in the international market condition of aviation geophysical prospecting and the remarkable development of the helicopter technology, the HTEM began to replace the FTEM as the mainstream solution of the ATEM system.

At present, the international mainstream HTEM systems (VTEM, SkyTEM, HeliTEM, etc.) have shown the features of multi-model serialization that takes into account the needs of deep and shallow exploration. The initial design trend of the VTEM system (Fig. 2a) of Geotech Ltd. is the large transmitter moment [6]. In 2011, the performance of early response detection was improved using system response correction for existing models, which so were upgraded to the ''full-wave''

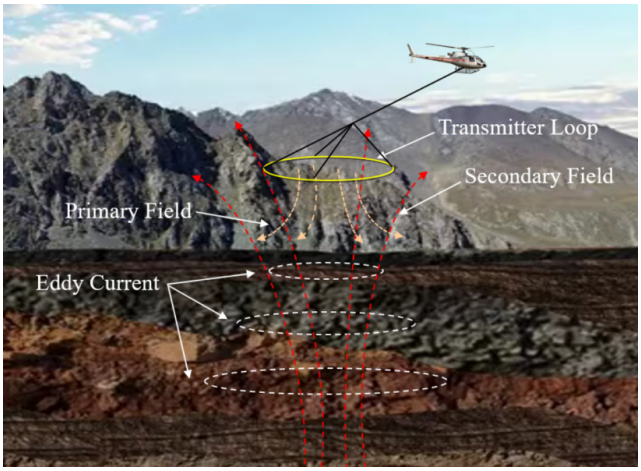

FIGURE 1. Schematic diagram of the ATEM method.

system [7]. In 2016, a new model VTEM ET system was further developed [8], which compressed the turn-off time from 1.3 ms to 500 μs, and increased the sampling rate from 192 kHz to 864 kHz. The pulse width and the amplitude of the transmitter current waveform can also be adjusted according to specific needs, so as to further enhance the ability of the VTEM series to detect the shallow target.

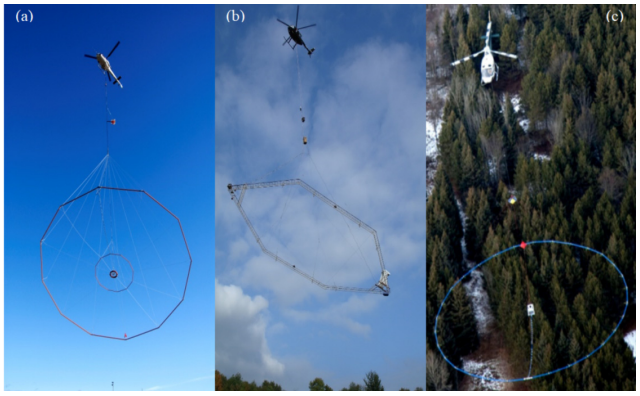

FIGURE 2. The international mainstream HTEM systems: (a) VTEM, (b) SkyTEM and (c) HeliTEM.

SkyTEM system (Fig. 2b) was developed with the support of the Danish national project to solve the problem of underground freshwater detection, so its original design goal was to enable shallow high-resolution detection [9]. SkyTEM is a dual magnetic moment system, which can change the number of turns of the transmitting coil through a special circuit, so that the system has a low moment mode (LM) and a high moment mode (HM). In order to improve the deep detection ability, the SkyTEM has further enhanced the peak moment of the HM mode. At present, the peak moment of the HM mode of the model SkyTEM-516 has reached about 1 MAm^2 [10], which is close to the peak moment of the former Fugro Company's FTEM system MEGATEM.

CGG's HeliTEM system (Fig. 2c) followed the relevant technologies of the former Fugro Company's FTEM systems, and its original design goal was also to achieve a large detection depth. In 2013, the Multi-Pulse technology [11] was introduced, and a short pulse with relatively low amplitude will be transmitted complementary at the end of the off-time period. This short pulse will increase the bandwidth of the entire transmitting signal and significantly improve the shallow detection capability of the system.

The central and western regions of China have appropriate conditions for mining development, but there are many deserts, swamps and forest-covered areas in this vast land. As a result, the traditional on-ground methods are difficult to carry out efficiently in these areas. The ATEM equipment and technology are urgently needed. In recent years, with the support of national projects, the Aero Geophysical Survey & Remote Sensing Center of Ministry of Land and Resources (AGRS), Jilin University, Chinese Academy of Sciences (CAS) and many other units have carried out the key technology research and system development, and two HTEM systems, CHTEM-I and CAS-HTEM, were developed in China. In this paper, the difficult issues in the development of HTEM hardware and software will be analyzed, firstly. By tracing the specific technical paths to solve these difficult issues, the latest research achievements in the development process of CHTEM-I and CAS-HTEM will be expounded. Finally, we would like to briefly discuss the research and development direction of HTEM technology in China to promote further development of the research and application of this technology.

II. DIFFICULTY ANALYSIS OF HTEM SYSTEM DESIGN

Generally, the earth is assumed to be a linear time-invariant system in transient electromagnetic (TEM) method [1]. Here, assuming that impulse response of the earth is $g(t)$, the function of the transmitting current pulse is $I(t)$, the induction magnetometer (IM) is used as sensor for observation of earth response, and the system functions of sensor and receiver are $h_S(t)$ and $h_R(t)$, respectively. The observed TEM signal is recorded as $V(t)$ and can be expressed as [1]:

$$V(t) = -S_T \cdot S_S \cdot g(t) * \frac{dI(t)}{dt} * h_S(t) * h_R(t) + n(t) \quad (1)$$

where S_T and S_S are the effective area of the transmitter loop and the induction magnetometer, respectively, $dI(t)/dt$ is the derivative waveform of the transmitting current pulse, $n(t)$ is the noise.

To achieve large detection depth, the transmitting end (transmitter + antenna) is required to provide a large moment, while the receiving end (receiver + sensor) is required to reach a low noise level as possible. However, to achieve a high detection resolution, the transmitting end is required to realize a rapid turn-off (so that the $dI(t)/dt$ has a large bandwidth), while the receiving end is required to have a large bandwidth and dynamic range. These requirements can be

well implemented for the ground system simultaneously, but for the airborne system, it will face the following difficulties:

A. DIFFICULTY IN TRANSMITTING END

The turn-off time is a key indicator to measure the shallow detection performance of the TEM system. The shorter the t_{off}, the larger the bandwidth of the excitation signal and the higher the detection accuracy that can be achieved. The t_{off} has the following relationship with the single-turn area of the transmitter loop A and the number of turns N of the transmitter loop [12]:

$$t_{off} \propto N^2 \cdot \sqrt{A} \tag{2}$$

This shows that t_{off} can be controlled more effectively by reducing the number of turns N. However, for HTEM systems, in order to ensure sufficient detection depth, it is necessary to realize a large transmitter moment on the transmitter loop carrier structure with a limited area, for this situation it is often only possible to increase the number of turns N, which in turn will lead to an increase in the off-time. Not only that, if the moment will be increased by increasing the current I, A and N individually or simultaneously, the system weight G will be also increased judging by formula (3) [12]:

$$G \propto \sqrt{A} \cdot N \cdot I^2 \tag{3}$$

It can be known from the comprehensive (2) and (3) that in order to achieve the optimal parameter design that takes into account the transmitting magnetic moment, the turn-off time and the system weight, the ideal choice is to increase the area A. However, increasing the area A will increase the overall size of the frame structure on which the transmitter loop is mounted. This will lead to an increase in system total weight, and may also increase the structural air resistance during flight, which will affect flight safety.

B. DIFFICULTY IN RECEIVING END

For HTEM systems, because the distance between the transmitter loop and the Sensor is relatively short, the primary field signal can easily cause the sensor to be deeply saturated. Because the desaturation process also requires time, this situation makes the data in the entire On-time period and the early stage of the Off-time period unavailable. The suppression of the primary field can be achieved through specific system designs, but it also puts forward higher requirements for the subsequent processing:

(1) Enlarging the offset between the transmitter loop and the sensor. This method generally sets the sensor away from the transmitter loop plane, such as a certain distance above the transmitter loop, so that the primary field weakens into the dynamic range of the sensor and no longer causes data saturation. This solution solves the problem of sensor saturation, but also increases the distance between the sensor and the ground, which requires a sensor with a lower noise level.

(2) Using compensation coil with opposing magnetic flux. The compensation coil, the transmitting coil, and the sensor have a concentric structure, and the compensation coil can generate a reverse magnetic flux of equal magnitude with the primary field at the sensor, to achieve the cancellation of the primary field. This solution requires higher assembly accuracy, otherwise, the reverse magnetic flux cannot accurately compensate the primary field, which results in the existence of the remaining primary field.

(3) Placing the sensor in the ''zero position''. The sensor coil is placed above the transmitter loop so that the positive and negative magnetic fluxes of the primary field passing through it cancel each other out. This method also requires higher assembly accuracy. When the determined zero position is inaccurate, it will also produce an effect similar to the previous mentioned remaining primary field.

The above analyses demonstrate that the HTEM system cannot be realized simply by aerial deployment of the traditional on-ground TEM system. Many external factors affect the performance of HTEM system, so its design is more difficult.

III. DEVELOPMENT OF HTEM SYSTEM IN CHINA

By continuously tracking the technological development of the international mainstream HTEM systems, multiple Chinese research teams have gradually launched the research and development of the HTEM system.

Since 2010, ARGS, Jilin University and many other units have jointly developed the CHTEM-I system with a rigid frame structure [13]. As shown in Fig. 3, CHTEM-I is a central loop system, the radius of transmitter loop is 6 m with 5 turns. The current waveform is a bipolar trapezoidal wave, the turn-off time is about 1.2 ms, the duty cycle is about 1:4.4, the peak transmitting current is 450 A (typical value is 400 A), and the peak moment is approximately is about 0.26 MAm^2. After further upgrades, the peak current has been raised to 500 A, and the turn-off time has been controlled within 1 ms.

FIGURE 3. CHTEM-I System [14].

Another team composed of CAS, Jilin University and many units has jointly developed the CAS-HTEM system with a soft frame structure, since 2013. As shown in Fig. 4, CAS-HTEM is also a central loop system, the peak transmitting current is 250 A (typical value is 210 A), the peak

FIGURE 4. CAS-HTEM system.

moment is about 0.7 MAm2, the turn-off time is about 450 μs, the noise level of the induction magnetometer is 0.1 nT/s. To increase the receiver's dynamic range, a double-gain channel strategy is adopted, which means inputting a signal into two channels with different amplification gains (1/4, 1, 2, 4, 8, 16), and then synthesizing them into one signal after amplification. The CAS-HTEM has six receiving channels (one group for every two), which allows for three-axis observation. In addition, to evaluate and correct the observation errors caused by flight attitude in the later stage, the system is equipped with many auxiliary sensors such as aerial camera, three-component attitude sensor, post-differential GPS, radar, and laser altimeter.

A. TRANSMITTER TECHNOLOGY

The trapezoid-like waves are used as transmitting current waveforms both in CHTEM-I and CAS-HTEM. The control of the current waveform is generally divided into rising and stable section control and falling edge control. It is required that the waveform of the rising and stable section should be stable, and the falling edge should be rapid and linear.

Based on BOOST circuit, Zhu *et al.* [15] introduced that by introducing active constant voltage clamping technology so that the transmitting current could be turn-off quickly and linearly under the conditions of high current transmitting and highly inductive load.

Yu *et al.* [16] adopted the soft switching technology based on Buck Zero-Current-Switching Pulse-Width-Modulation (ZCS-PWM) instead of the traditional hard switching technology that only relies on PWM. The soft switching technology could effectively control the rising and stable waveforms of the current waveform, reduce the switching losses, noise and ripple, and further reduce power.

To meet the requirements of mounting on the flight platform, Li *et al.* [17] introduced a three phases - single phase matrix converter to replace the traditional system based on AC/DC converter and H bridge inverter, which is helpful to further reduce the weight of the transmitter.

In the early stage of CAS-HTEM system development, an airship-borne TEM system was developed for system principle verification, for which a double-hull airship was used as platform. As shown in Fig. 5, the transmitter loop of the airship-borne TEM system was fixed on the bottom of the airship, with a single turn of 25m$\times$12m and six turns. A three-axis induction magnetometer was used as the sensor, which was suspended in a pod approximately 25m below the transmitter loop. The airship-borne TEM system adopted a half-sine transmitting waveform. Liu *et al.* [18] completed the development of the transmitter based on the proposed bipolar half-sine current inverter topology based on RLC series resonance and damping resistor pairs. With onboard 28V DC power supply, this transmitter achieved a peak current of more than 500 A.

FIGURE 5. Airship-borne TEM system.

B. SENSOR TECHNOLOGY

The noise level and the bandwidth of the linear frequency response curve are the two most critical parameters of the induction magnetometer (IM) for TEM. Liu *et al.* [19] summarized the existing design experience of IM for TEM, discussed the relationship between the sensor linear frequency response and under-damped matching, and proposed the main factors that affect the performance of the sensor at different frequency bands. To meet the requirements of mounting on the flight platform, Duan and Luo [20] proposed an adaptive

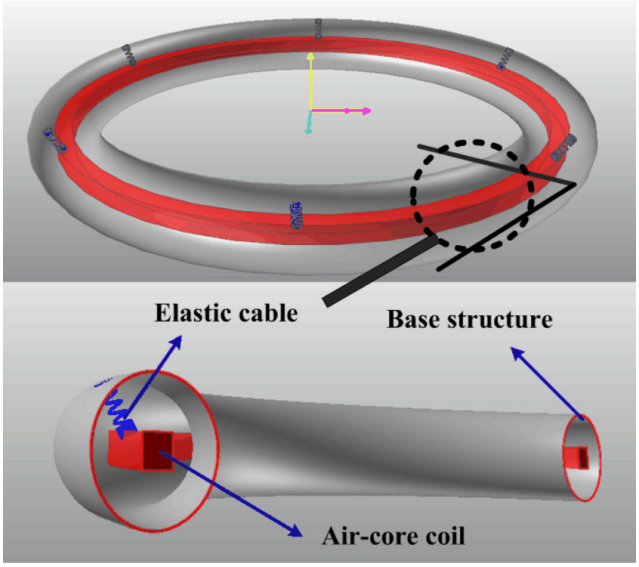

FIGURE 6. Simulation model of the CPS [21]. The CPS is a six-degree-of-freedom system; calculating and selecting the elastic cable's setting position and performance parameters allows for effective intervention on IM's natural mechanical frequency range.

algorithm based on the Backtracking search algorithm, which is helpful to further optimize the weight and volume of IM. Motion-induced noise (MIN) is an important type of noise in ATEM detection. Fei *et al.* [21] considered a special system structure including cable parallel structure (CPS) and air-core IM. As shown in Fig. 6, CPS is used to change the natural mechanical frequency range of the air-core IM. In this way, the MIN generated by the IM vibration could be separated from the useful signals in the frequency spectrum, so that the MIN is removed by filtering more easily. In recent years, Ji *et al.* [22] and Du *et al.* [23] used LT-SQUID to carry out ground TEM detection and research of IP effect in TEM. These research and application work laid the foundation for the future development of HTEM systems based on LT-SQUID.

C. TEST SITE

In order to test and evaluate the detection performance of the developed equipment, many geological survey institutions worldwide have built their own aero-geophysical static and dynamic test bases [24]. In China, there was only an airborne energy spectrum instrument metering station and calibration band in Shijiazhuang built by the Airborne Survey and Remote Sensing Center of Nuclear Industry (ASRS) before 2012. Afterward, the methods for selecting and constructing the aero-geophysical field test site have been established and improved by AGRS [25], and subsequently the comprehensive aero-geophysical field test site in north China has been established [26]. The test site is located in Siziwang Banner, Inner Mongolia, approximately 31.5km from north to south and 31.8km from east to west. The general elevation of the test site is 1350-1550m above sea level. The area has many mineralization points of iron, gold, copper, and tungsten. The maximum amplitude of the magnetic anomaly is $>$ 100 nT, and the maximum amplitude of the gravity anomaly is $>$ 20 mGal. The test area is far from the town, and human noise is low. The completion of the test site will provide vital support to the development of airborne geophysical exploration technology, including HTEM.

IV. HTEM METHOD RESEARCH IN CHINA

A. DATA PROCESSING

The main task of HTEM hardware design is to optimize the detection performance of the system under the conditions of limited power supply and carrying capacity of the flight platform, while the main task of the HTEM data processing is to overcome various interferences and limitations brought by aerial observation, including: (1) Suppression of various noises, (2) Correction of attitude effects, and (3) ''Remedy'' of performance defects of hardware systems introduced by adaptive system design for aerial observation.

1) DENOISING

Research by Combrinck [27] demonstrates that when the system noise level drops by approximately 12 dB, the maximum detectable depth of the system can be increased by about 100 meters, so the noise suppression is of great significance to improve the detection performance of the system. According to the source, the noise entering the HTEM data can be roughly divided into internal noise and external noise [28]. The internal noise mainly comes from the hardware system, especially from the amplification circuit of the IM. The external noise mainly includes: Natural EM noise, Cultural EM noise, and motion-induced noise (MIN). The bipolar synchronous sampling method in the traditional TEM is still the most important noise suppression strategy in HTEM. However, because the observation position changes continuously with time during the measurement, so it is impossible to achieve noise suppression for HTEM through long periods of observation and data superposition, as the ground method does. Therefore, new noise processing methods need to be introduced.

Because the MIN is considered exclusive to ATEM, while other noises (non-MIN noises) occur in both airborne and ground TEM. To achieve the fine removal of non-MIN noise, the common methods at present can be summarized as ''Decomposition of observation signal-Removal of noise component-Reconstruction of useful signal (DRR)''. Chen *et al.* [29] proposed a denoising method based on kernel principal component analysis, in which the kernel principal component analysis will be used to transform the observation data into the kernel principal component domain. In the kernel principal component domain, the useful signal and noise will be separated, and then the noise will be removed by reconstructing only the useful signal. For denoising along with the channel profile, Wang *et al.* [30] introduce the adaptive window wide-filter algorithm to design different

component low-pass filter groups, so that in the principal component domain, the noise in the low-order principal components participating in the profile reconstruction could be filtered out. Zhu *et al.* [31] proposed a denoising method based on minimum noise fraction, which linearly transforms the observation data into the ''minimum noise fraction component domain'' through the rotation matrix, in which the components are arranged in signal to noise ratio from big to small, then the minimum noise fraction components with the bigger SNR will be used for the useful signal reconstruction. Ji *et al.* [32] proposed a denoising method based on the stationary wavelet transform, which transforms observation data into the wavelet domain, and then the wavelet threshold method will be used to separate the useful signal and noise.

In order to remove the MIN, there are two kind of traditional methods, the high-pass filtering and the MIN fitting. Wang *et al.* [33] studied the filtering scheme, discussed the relationship between the sensor attitude and motion state with MIN, and designed a more precise filter to improve the filtering effect. In view of the shortcomings of the traditional high-pass filtering method, Yin *et al.* [34] used the curve fitting method: the coefficients of the MIN fitting polynomial will be solved using the Lagrange optimization algorithm, and then the MIN will be removed by subtracting the high-quality fitted noise curve from the measured data. During normal flight, if the sensor bird encounters short-term turbulence or the system's flight state changes rapidly, these sudden conditions will cause high-frequency MIN. The frequency range of high-frequency MIN is several hundred Hz to several kHz, and far higher than the normal MIN. The high-frequency MIN is therefore a serious in-band noise in HTEM data. Wu *et al.* [35] proposed a processing flow based on the wavelet neural network, which use the wavelet neural network to realize the effective modeling and prediction of high frequency MIN, so as to realize the accurate removal of it. In addition, Zhu *et al.* [36] demonstrated that in addition to the main source of MIN, the movement of the normal vector of the coil in the secondary field also leads to MIN in the region with a strong secondary field. The conclusion of this study constituted the theoretical premise of the aforementioned work by Fei *et al.* [21].

2) COIL ATTITUDE CORRECTION

In HTEM flight, due to the adjustment of the flight state and the influence of the air flow, the transceiver system will roll (spin around the X-axis), pitch (spin around the Y-axis) and yaw (spin around the Z-axis), and resulting in some degree of data distortion. Because the HTEM transceiver structure is typically Z-axis-symmetric, the yaw has relatively little impact on the system with only Z-axis observation, and it is also relatively uncomplicated to correct the data impact caused by roll and pitch due to the fixed internal geometry of the HTEM transceiver system. Ji *et al.* [37] proposed a method for attitude correction, and provided theoretical guidance for designing the installation position of the attitude, altitude, and position sensors in the subsequent CAS-HTEM system. Based on the research of Auken *et al.* [38], and to further ensure the effectiveness of the correction, the CAS-HTEM system requires that the roll angle and pitch angle should not be greater than $\pm 10^{\circ}$ in the actual flight. In addition, the specification of the CAS-HTEM system also requires that when the number of measuring points with roll angle and pitch angle greater than $\pm 10^{\circ}$ accounts for more than 5% of the total measuring points in a survey line, re-measuring must occur for this line.

3) REMOVAL OF SYSTEM RESPONSE EFFECT

The system response effect refers to the band-limited effect of the HTEM observation system on the earth response. As demonstrated in (1), observing dI(t)/dt and deconvoluting it out from V (t) will effectively increase the signal bandwidth and improve the ability to resolve shallow target. Through this technology, the excitation signal bandwidth can be ''patched'' to a certain extent [7]. Dring data processing for the CAS-HTEM system, the transmitter current waveform of the high-flight segment is taken as standard. In this way, although the current waveforms in the actual observation are not completely consistent, we use the deconvolution technology to normalize all the real observation data to the data generated by this standard current waveform. With this special reference, even if the transceiver system generates a certain remaining primary field in the data due to insufficient assembly accuracy, the system response can be removed accurately. As a result, the earliest available time point advances to the level of $n \times 10$ μs, which significantly improves the system's resolution to the shallow part. In addition, Xiao *et al.* [39] propose a method to transform the observed data and transmitter waveform to the time-constant domain, and remove the band-limited effect in the time constant domain, which further improves the processing efficiency.

B. IMAGING

After the data processing, imaging and inversion well be used to obtain the distribution information of the subsurface electrical structure. In essence, imaging is one kind of mathematical transformation for the observation data, which needs no curve fitting based on the optimization algorithm. The imaging can therefore directly obtain the intermediate parameters such as the apparent resistivity and apparent depth of the earth. On the basis of the existing imaging algorithm, Qi *et al.* [40] introduced a new imaging method based on the idea of a synthetic aperture. In this method, the correlation coefficients of signals at different measurement points will be calculated to generate different weight functions. These weight functions will be taken as references, when the adjacent signal points are superimposed and formed new data, so as to realize the relevant superimposition of HTEM data for fast imaging (Fig. 7). To obtain better imaging effect and resolution, Zhu *et al.* [41] proposed that the combination of Bx and Bz observations for conductivity-depth imaging can achieve a better agreement with the true model. For different transmitter loop devices, Qin *et al.* [42] established

the mapping relationship between TEM response characteristics and resistivity based on the artificial neural network. After well training, the network could be directly used for TEM resistivity imaging, which significantly improves the processing speed.

C. MODELING

In electromagnetic forward modeling research, the main methods used include Finite Difference Time Domain (FDTD), Finite-Element (FE), Finite-Volume (FV) and Time-Domain Spectral-Element (SETD). Sun *et al.* [43] proposed an FDTD method based on a multi-scale grid. This method first uses a coarse grid for large-scale calculations, and then performs a secondary division of the desired encrypted area, thereby significantly improving the calculation efficiency on the basis of ensuring the calculation accuracy. Zhao *et al.* [44] adopted the first two initial times of electric field and second initial time of ∂B/∂t as initial conditions to improve initial precision; in subsequent iterations, the electric fields and ∂B/∂t are both valued at the same integer time indices, thus iteration precision will be further improved. To further improve the efficiency and accuracy of FE calculations, Zhang *et al.* [45] proposed an adaptive unstructured mesh-generation method based on the backward Euler scheme, hybrid posterior error estimation and random grid-selection technique, and these enable a fast calculation of AEM response in large-scale, complex target spaces. Li *et al.* [46] proposed a forward-solver based on FE for the irregular transmitter loop and undulating terrain. Compared with FDTD and FE, the FV method can balance the advantages of both to a certain extent. Ren *et al.* [47] used the FE to develop ATEM 3D modeling, which involves separating the primary and secondary fields to reduce the number of grids, as well as using local grid technology and direct solution technology to further improve FE modeling efficiency. In addition, Huang *et al.* [48] developed a SETD method based on the mixed order spectral-element approach for space discretization and the backward Euler approach for time discretization, and adopted this method in the 3D modeling of ATEM. The above-mentioned research has significantly promoted the development of ATEM modeling in China.

D. INVERSION

HTEM inversion can be divided into one-dimensional inversion and multi-dimensional inversion. Lin *et al.* [49] proposed a robust scheme based on the laterally constrained inversion [50] algorithm, which considers the induced polarization effect. Li *et al.* [51] proposed an inversion method based on the Bayesian framework for decoupling the IP effect, which adopts linear inversion results as the initial model and adopts the multiple proposed points algorithm for sampling acceleration to realize IP decoupling inversion for TEM data. In terms of descent direction searching, Yin and Hodges [52] proposed a method using the simulated quenching method. Guo *et al.* [53] proposed an inversion method based on the supervised descent method, which is a method to select the inverse descent direction by machine learning method. In addition, Zhu *et al.* [54] proposed an artificial neural network (ANN) inversion method based on the principal components of the decay curve. The basic principle of this method is to decompose the observed data into principal components and use ANN to communicate the principal components and model parameters to realize the inversion of the subsurface resistivity model.

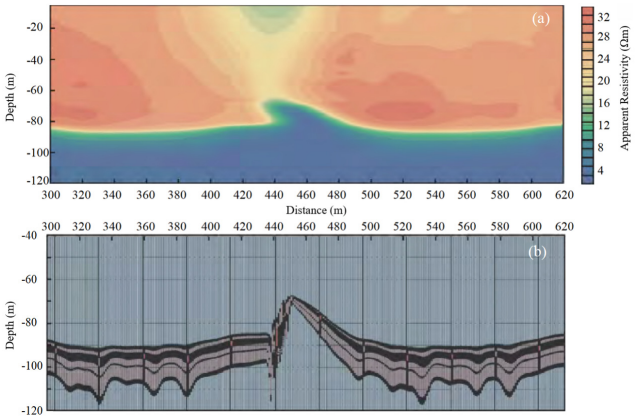

FIGURE 7. Results of measured data [40]. (a) Apparent resistivity section; (b) section calculated using synthetic aperture method.

In terms of multi-dimensional inversion, Yang and Oldenburg [55] proposed a three-dimensional inversion workflow based on the multi-mesh strategy, and this strategy effectively improves inversion efficiency and demonstrates that the multi-dimensional inversion can provide more precise extraction of geological structure information. For the multipulse technology of the HeliTEM system, Liu and Yin [56] developed a three-dimensional multipulse inversion method based on the FD, Gauss-Newton optimization and moving footprint technology. Ren *et al.* [57] proposed a three-dimensional inversion method based on FV and direct Gauss-Newton optimization, and their method controls the modeling volume in the AEM volume of influence of a 3D source within the earth, which alleviates forward calculation stress.

V. HTEM APPLICATION IN CHINA

The application of the HTEM technology in China is still in its primary stage. Li *et al.* [58] introduced the experimental detection activities of ASRS using the VTEM system in Xinjiang and Inner Mongolia. The detection results are consistent with prior data. Since then, ASRS has organized metal exploration activities in Qinghai Province [59] and Heilongjiang Province [60], which all have achieved reasonable results. The Wulonggou survey area in Qinghai is located on the northern side of the arc-magmatic-metamorphic complex zone in the central margin of Kunming and the Kunzhong fault zone. This zone is characterized by a large area of Precambrian base metamorphic rock series and intrusive

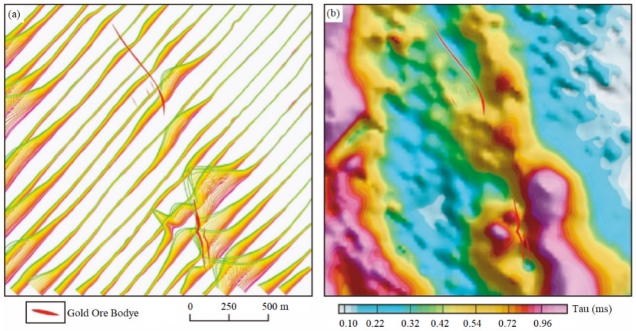

FIGURE 8. Results of airborne electromagnetic and magnetic survey in the mining area [59]. (a) Profiles map of dB/dt (30 ∼ 45); (b) map of time constant. The electromagnetic response in the measurement area is characterized by east-west sub-zoning. As Figure (a) demonstrates, the gold ore body has obvious double-peak characteristics, with the right peak higher than the left; as Figure (b) demonstrates, the gold ore body is located in a relatively low-value zone in the middle of the high-value zone and has a higher value on the east side.

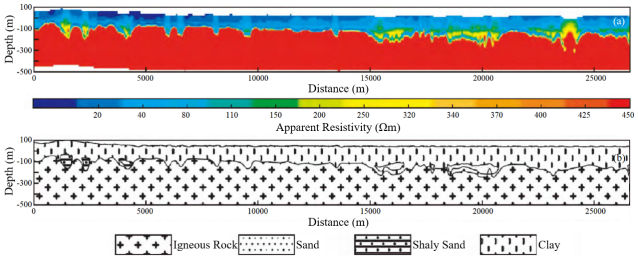

FIGURE 9. Result profiles of one survey line in Baoqing area [61]. (a) Apparent resistivity profile; (b) geological interpretation along the survey line.

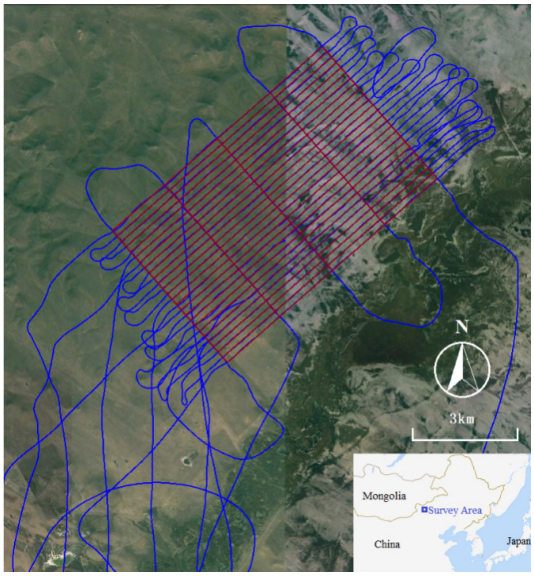

FIGURE 10. Designed survey line and tracks of CAS-HTEM test flight.

complexes of various ages. The strata are generally distributed along the Kunzhong and Northern Kunshan fault zones, and magmatic invasion occurred in Eastern Europe from the Precambrian to Yanshan period. In the Wulonggou gold mine, the airborne electromagnetic and magnetic surveying have been carried out. By studying the results of electromagnetic detection (Fig. 8) and combining prior geological data, six targets were delineated in the mining area, and one has been verified by drilling.

The CHTEM-I system was used for detection in Keshiketeng Banner, Inner Mongolia, and 40 electromagnetic anomalies were found. At present, two anomalies have been tested by drilling. In Hami, Xinjiang Province, 38 electromagnetic anomalies were discovered. Through ground inspection, Baoyuandong copper-nickel or copper mineralization and Hongliuchuan gold deposit were newly tested.

In addition to exploring mineral resources, AGRS also conducts hydrogeological surveys using HTEM technology. In the exploration of Baoqing County [61] and the Fujin-Youyi area [62], Heilongjiang Province, AGRS found that the regional quaternary electrical distribution characteristics and the depth of the bottom surface can be clearly delineated. By establishing a three-dimensional geological model, the lithology can be inferred and the distribution of aquifers can be predicted. The Baoqing County survey area is 28 km wide from north to south and 32.6 km long from east to west; 66 north-south survey lines are arranged at 500m line distance.

Figure 9 depicts the apparent resistivity section of one of the survey lines and the inferred geological section. The apparent resistivity section clearly demonstrates the high-resistance bedrock and the relatively high-resistance areas in the low-resistance area. Combining a priori geological information, the general apparent resistivity is in the range of 90-150 Ωm, and the areas with low-resistance areas in the upper and lower parts are bodies of water. The upper low-resistance area is interpreted as clay, the base is igneous rock, the relatively high-resistance piece in the low-resistance area is the aquifer sand layer, and the next high-resistance area of clay near the igneous rock is muddy sand.

CAS completed the research and development of the CAS-HTEM system in 2017 and conducted a principle verification test in East Wuzhumuqin Banner, Inner Mongolia, north China. The detection results were consistent with prior data, and new mineralization anomalies were found. As shown in Fig. 10, 29 North-South survey lines (8.5 km line length, 200 m line spacing) and five East-West lines (5.6 km line length, 2 km line spacing) were designed. Fig. 11 provides the slice map with drill holes No. 6 and No. 9 of the survey area. High-grade mineralization was observed in borehole 6, while in borehole 9, the degree of mineralization was low. CAS-HTEM inversion results in a high-low resistance transition zone in the borehole 6 area and a pure high-resistance zone in borehole 9. Using the above detection results as reference, new mineralization anomalies were found in the survey area.

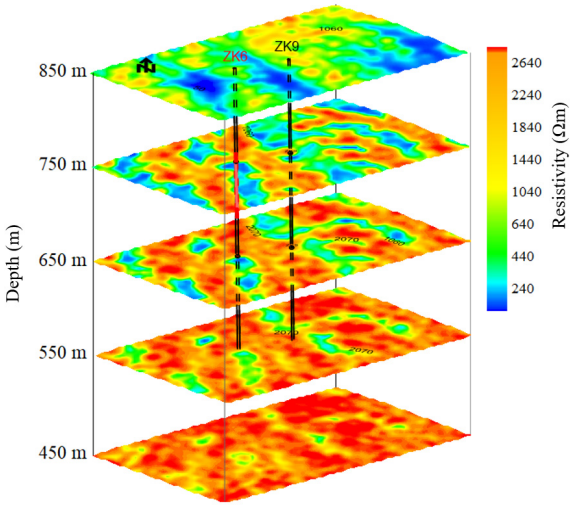

FIGURE 11. Slice map with drill holes No. 6 and No. 9.

VI. PROSPECTS AND CONCLUSION

Since 2016, China has made significant progress in the development of HTEM equipment and technology research, but a large number of practical problems remain. These problems include the need to develop systems with ultra-large magnetic moment (over 1.5 MAm^2) to suit large depth detection in the plains, and systems with a medium magnetic moment in plateau and mountainous areas. Novel sensors such as SQUID and non-contact electric field sensors could be introduced in airborne electromagnetic detection. The focus on data processing and interpretation is to further develop rapid high-dimensional imaging and inversion techniques. The HTEM data will be integrated into a larger geoscience information system architecture for the comprehensive geophysical interpretation.

Gradually achieving the above-mentioned key technologies will promote the development and application of China's ATEM detection equipment and provide more powerful technical means for resource detection and engineering construction.

REFERENCES

[1] M. N. Nabighian, Ed., *Electromagnetic Methods in Applied Geophysics: Theory*, vol. 1. Tulsa, OK, USA: Society of Exploration Geophysicists, 1988.

[2] A. P. Annan and R. Lookwood, "An application of airborne Geotem in Australian conditions," *Explor. Geophys.*, vol. 22, no. 1, pp. 5–12, Mar. 1991.

[3] R. S. Smith, A. P. Annan, J. Lemieux, and R. N. Pedersen, "Application of a modified GEOTEM system to reconnaissance exploration for kimberlites in the Point Lake area, NWT, Canada," *Geophysics*, vol. 61, no. 1, pp. 82–92, Jan. 1996.

[4] K. Witherly, R. Irvine, and M. Godbout, "Reid Mahaffy test site, Ontario Canada: An example of benchmarking in airborne geophysics," in *Proc. 74th Annu. Int. Meeting, Soc. Explor. Geophysicists*, Denver, CO, USA, Oct. 2004, pp. 1202–1204.

[5] K. I. Sorensen and E. Auken, "SkyTEM—A new high-resolution helicopter transient electromagnetic system," *Explor. Geophys.*, vol. 35, no. 3, pp. 194–202, Sep. 2004.

[6] K. Witherly, R. Irvine, and E. Morrison, "The Geotech VTEM time domain helicopter EM system," in *Proc. 74th Annu. Int. Meeting, Soc. Explor. Geophysicists*, Denver, CO, USA, Oct. 2004, pp. 1217–1220.

[7] J. M. Legault, A. Prikhodko, D. J. Dodds, J. C. Macnae, and G. A. Oldenborger, "Results of recent VTEM helicopter system development testing over the spiritwood valley aquifer, Manitoba," in *Proc. Symp. Appl. Geophys. Eng. Environ. Problems (SAGEEP)*, Tucson, AZ, USA, Mar. 2012, pp. 114–130.

[8] T. Eadie, M. Legault, G. Plastow, A. Prikhodko, and P. Tishin, "An improved helicopter time-domain EM system for near surface applications," in *Proc. Near Surface Geosci. 17th Conf. Exhib.*, Malmö, Sweden, Sep. 2017.

[9] K. I. Sørensen and E. Auken, "New developments in high resolution airborne TEM instrumentation," in *Proc. 16th Geophys. Conf. Exhib., Austral. Soc. Explor. Geophysicists*, Adelaide, SA, Australia, Feb. 2003, pp. 1–4.

[10] F. Effersoe and B. Brown, "Application of helicopter time-domain EM for mine operations," in *Proc. Near Surface Geosci. 17th Conf. Exhib.*, Malmö, Sweden, Sep. 2017.

[11] T. Chen, G. Hodges, and P. Miles, "MULTIPULSE—High resolution and high power in one TDEM system," *Explor. Geophys.*, vol. 46, no. 1, pp. 49–57, Mar. 2015.

[12] P. V. Kuzmin and E. B. Morrison, "Large airborne time-domain electromagnetic transmitter coil system and apparatus," U.S. Patent 7 948 237 B2, May 24, 2011.

[13] S.-J. Liang, L.-K. Zhang, X.-F. Cao, and Q.-K. Liu, "Research progress of the time-domain airborne electromagnetic method," *Geol. Explor.*, vol. 50, no. 4, pp. 735–740, Jul. 2014.

[14] X.-F. Cao, *The Subproject of 863 Project 'Practical Research on Helicopter Time-Domain Electromagnetic Exploration System' Has Successfully Passed the Acceptance of the Center*. Accessed: Dec. 19, 2016. [Online]. Available: http://www.agrs.cn/dydt/cgkx/17026.htm

[15] X. Zhu, X. Su, H.-M. Tai, Z. Fu, and C. Yu, "Bipolar steep pulse current source for highly inductive load," *IEEE Trans. Power Electron.*, vol. 31, no. 9, pp. 6169–6175, Sep. 2016.

[16] S.-B. Yu, J. Jiang, C.-Y. Sun, and X. Cheng, "Research on novel pulse current emission circuit for airborne transient electromagnetic method," *J. Central South Univ. (Sci. Technol.)*, vol. 48, no. 9, pp. 2388–2395, Sep. 2017.

[17] G. Li, S.-B. Yu, S.-H. Jia, and Q.-J. Wang, "Control of three phases—Single phase matrix converter for transient electromagnetic sounding," in *Proc. 17th Int. Conf. Electr. Machines Syst. (ICEMS)*, Oct. 2014, pp. 3074–3077.

[18] L. Liu, Z. Shi, K. Wu, Z. Geng, and G. Fang, "A bipolar half-sine current inverter for airship-borne electromagnetic (AEM) surveying," *IEEE Trans. Ind. Electron.*, vol. 64, no. 12, pp. 9477–9486, Dec. 2017.

[19] K. Liu, X.-L. Mi, W.-H. Zhu, B. Yan, L.-S. Liu, and G.-Y. Fang, "A design of high sensitivity induction magnetometer for TEM," *Chin. J. Geophys.*, vol. 57, no. 10, pp. 3485–3492, Oct. 2014.

[20] H. Duan and Q. Luo, "Adaptive backtracking search algorithm for induction magnetometer optimization," *IEEE Trans. Magn.*, vol. 50, no. 12, pp. 1–6, Dec. 2014.

[21] L. Fei, J. Lin, Y.-Z. Wang, S.-L. Wang, X.-F. Cao, and B. Chen, "Design of cable parallel air-core coil sensor to reduce motion-induced noise in helicopter transient electromagnetic system," *IEEE Trans. Instrum. Meas.*, vol. 68, no. 2, pp. 525–532, Feb. 2019.

[22] Y. Ji, S. Du, L. Xie, K. Chang, Y. Liu, Y. Zhang, X. Xie, Y. Wang, J. Lin, and L. Rong, "TEM measurement in a low resistivity overburden performed by using low temperature SQUID," *J. Appl. Geophys.*, vol. 135, pp. 243–248, Dec. 2016.

[23] S. Du, Y. Zhang, Y. Pei, K. Jiang, L. Rong, C. Yin, Y. Ji, and X. Xie, "Study of transient electromagnetic method measurements using a superconducting quantum interference device as B sensor receiver in polarizable survey area," *Geophysics*, vol. 83, no. 2, pp. E111–E116, Mar. 2018.

[24] R. S. Smith, L.-Z. Cheng, M. Allard, M. Chouteau, P. Keating, J. Lemieux, M. A. Vallée, D. Fountain, and D. Bois, "An analysis of geophysical and geological data from the Gallen test site, Quebec, Canada," in *Proc. 76th Soc. Explor. Geophysicists Annu. Meeting*, Jan. 2006, pp. 1243–1247.

[25] W.-P. Zhu, S.-Q. Xiong, Y.-H. Liu, D.-J. Xue, X.-Z. Yue, and W. Zhang, "Selection principles and methods of Dajingpo airborne geophysical test site," *Geophys. Geochem. Explor.*, vol. 37, no. 1, pp. 98–103, Feb. 2013.

[26] W.-P. Zhu, S.-Q. Xiong, Y.-H. Liu, D.-J. Xue, G.-S. Wang, W. Zhang, and X.-Z. Yu, "Construction methods of China airborne geophysical field test site," *Progr. Geophys.*, vol. 29, no. 2, pp. 895–901, Feb. 2014.

[27] M. Combrinck, "The impact of AEM receiver noise levels on detection, discrimination and resolvability of conductive targets," in *Proc. 21st Int. Geophys. Conf. Exhib., Austral. Soc. Explor. Geophysicists*, Sydney, NSW, Australia, Aug. 2010.

[28] J. C. Macnae, Y. Lamontagne, and G. F. West, "Noise processing techniques for time-domain EM systems," *Geophysics*, vol. 49, no. 7, pp. 934–948, Jul. 1984.
[29] B. Chen, C.-D. Lu, and G.-D. Liu, "A denoising method based on kernel principal component analysis for airborne time domain electromagnetic data," *Chin. J. Geophys.*, vol. 57, no. 1, pp. 295–302, Jan. 2014.
[30] L.-Q. Wang, B.-B. Li, J. Lin, B. Xie, Q. Wang, Y.-Q. Cheng, and K.-G. Zhu, "Noise removal based on reconstruction of filtered principal components," *Chin. J. Geophys.*, vol. 58, no. 8, pp. 2803–2811, Aug. 2015.
[31] K.-G. Zhu, Y. Li, Y. Meng, L.-Q. Wang, B. Xie, and Y.-G. Cheng, "Application of minimum noise fraction on noise removal for airborne electromagnetic data," *J. Jilin Univ. (Earth Sci. Ed.)*, vol. 46, no. 3, pp. 876–883, May 2016.
[32] Y. Ji, D. Li, G. Yuan, J. Lin, S. Du, L. Xie, and Y. Wang, "Noise reduction of time domain electromagnetic data: Application of a combined wavelet denoising method," *Radio Sci.*, vol. 51, no. 6, pp. 680–689, Jun. 2016.
[33] Y.-Z. Wang, R. Smith, K.-G. Zhu, J. Lin, and B. Chen, "HTEM noise frequency characteristics simulation and influencing analysis," in *Proc. Int. Workshop Gravity, Electr. Magn. Methods Their Appl. (GEM Chengdu)*, Chengdu, China, Apr. 2015, pp. 398–401.
[34] D.-W. Yin, J. Lin, K.-G. Zhu, Y.-R. Wang, and B.-B. Li, "Simulation research on coil motion noise removal for time domain airborne electromagnetic data," *J. Jilin Univ. (Earth Sci. Ed.)*, vol. 43, no. 5, pp. 1639–1645, Sep. 2013.
[35] X. Wu, G.-Q. Xue, P. Xiao, J.-T. Li, L.-H. Liu, and G.-Y. Fang, "The removal of the high-frequency motion-induced noise of helicopter-borne transient electromagnetic data based on wavelet neural network," *Geophysics*, vol. 84, no. 1, pp. K1–K9, Jan. 2019.
[36] K.-G. Zhu, C. Peng, H. Wang, Q. Zhang, and Y.-M. Lu, "Numerical simulation of coil motion noise in airborne time-domain electromagnetic survey," in *Proc. 87th Annu. Meeting Soc. Explor. Geophysicists Int. Expo.*, Houston, TX, USA, Sep. 2017, pp. 1106–1109.
[37] Y.-J. Ji, J. Lin, S.-S. Guan, S.-B. Yu, and Y.-F. Gong, "Theoretical study of concentric loop coils attitude correction in helicopter-borne TEM," *Chin. J. Geophys.*, vol. 53, no. 1, pp. 171–176, Jan. 2010.
[38] E. Auken, M. Halkjœr, and K. I. Sørensen, "SkyTEM—Data processing and a survey," in *Proc. Symp. Appl. Geophys. Eng. Environ. Problems (SAGEEP)*, Denver, CO, USA, 2004, pp. 109–120.
[39] P. Xiao, X. Wu, Z.-Y. Shi, J.-T. Li, L.-H. Liu, and G.-Y. Fang, "Helicopter TEM parameters analysis and system optimization based on time constant," *J. Appl. Geophys.*, vol. 150, pp. 84–92, Mar. 2018.
[40] Z.-P. Qi, X. Li, J.-L. Guo, H.-F. Sun, W.-H. Wei, and Q. Wu, "Fast imaging of correlation stack for airborne TEM based on differential conductance," *Progr. Geophys.*, vol. 30, no. 4, pp. 1903–1911, Aug. 2015.
[41] K.-G. Zhu, B.-B. Li, Q. Wang, and Y.-Q. Cheng, "Joint conductivity-depth imaging for fixed-wing electromagnetic data Bx and Bz," in *Proc. Int. Workshop Gravity, Electr. Magn. Methods Their Appl.*, Chengdu, China, Apr. 2015, pp. 334–337.
[42] S. Qin, Y. Wang, Z. Xu, X. Liao, L. Liu, and Z. Fu, "Fast resistivity imaging of transient electromagnetic using ANN," *IEEE Geosci. Remote Sens. Lett.*, vol. 16, no. 9, pp. 1373–1377, Sep. 2019.
[43] H.-F. Sun, M. Cheng, Q.-L. Wu, D.-C. Mi, S.-C. Li, X. Li, D.-R. Li, K. Li, and J.-H. Luo, "A multi-scale grid scheme in three-dimensional transient electromagnetic modeling using FDTD," *Chin. J. Geophys.*, vol. 61, no. 12, pp. 5096–5104, Dec. 2018.
[44] X. Zhao, Y. Yu, Y. Ji, and H. Luan, "An improved finite-difference time-domain solution for three-dimensional transient electromagnetic modeling in source-free media," *Radio Sci.*, vol. 54, no. 11, pp. 975–985, Nov. 2019.
[45] B. Zhang, C. Yin, X. Ren, Y. Liu, and Y. Qi, "Adaptive finite element for 3D time-domain airborne electromagnetic modeling based on hybrid posterior error estimation," *Geophysics*, vol. 83, no. 2, pp. WB71–WB79, Mar. 2018.
[46] J.-H. Li, X.-S. Lu, C. G. Farquharson, and X.-Y. Hu, "A finite-element time-domain forward solver for electromagnetic methods with complex-shaped loop sources," *Geophysics*, vol. 83, no. 3, pp. E117–E132, May 2018.
[47] X.-Y. Ren, C.-C. Yin, Y.-H. Liu, J. Cai, C. Wang, and F. Ben, "Efficient modeling of time-domain AEM using finite-volume method," *J. Environ. Eng. Geophys.*, vol. 22, no. 3, pp. 267–278, Sep. 2017.
[48] X. Huang, C.-C. Yin, C. G. Farquharson, X.-Y. Cao, B. Zhang, W. Huang, and J. Cai, "Spectral-element method with arbitrary hexahedron meshes for time-domain 3D airborne electromagnetic forward modeling," *Geophysics*, vol. 84, no. 1, pp. F37–F46, Jan. 2019.
[49] C.-H. Lin, G. Fiandaca, E. Auken, M. A. Couto, and A. V. Christiansen, "A discussion of 2D induced polarization effects in airborne electromagnetic and inversion with a robust 1D laterally constrained inversion scheme," *Geophysics*, vol. 82, no. 2, pp. E75–E88, Mar. 2019.
[50] E. Auken and A. V. Christiansen, "Layered and laterally constrained 2D inversion of resistivity data," *Geophysics*, vol. 69, no. 3, pp. 752–761, May 2004.
[51] H. Li, G. Xue, and Y. He, "Decoupling induced polarization effect from time domain electromagnetic data in a Bayesian framework," *Geophysics*, vol. 84, no. 6, pp. A59–A63, Nov. 2019, doi: 10.1190/geo2019-0247.1.
[52] C.-C. Yin and G. Hodges, "Simulated annealing for airborne EM inversion," *Geophysics*, vol. 72, no. 4, pp. F189–F195, Jul. 2007.
[53] R. Guo, M.-K. Li, F. Yang, S.-H. Xu, G.-Y. Fang, and A. Abubakar, "Application of gradient learning scheme to pixel-based inversion for transient EM data," in *Proc. IEEE Int. Conf. Comput. Electromagn.*, Mar. 2018, pp. 1–3, doi: 10.1109/COMPEM.2018.8496518.
[54] K.-G. Zhu, M.-Y. Ma, H.-W. Che, E.-W. Yang, Y.-J. Ji, S.-B. Yu, and J. Lin, "PC-based artificial neural network inversion for airborne time-domain electromagnetic data," *Appl. Geophys.*, vol. 9, no. 1, pp. 1–8, Mar. 2012.
[55] D. Yang and D. W. Oldenburg, "Three-dimensional inversion of airborne time-domain electromagnetic data with applications to a porphyry deposit," *Geophysics*, vol. 77, no. 2, pp. B23–B34, Mar. 2012.
[56] Y. Liu and C. Yin, "3D inversion for multipulse airborne transient electromagnetic data," *Geophysics*, vol. 81, no. 6, pp. E401–E408, Nov. 2016.
[57] X.-Y. Ren, C.-C. Yin, J. Macnae, Y.-H. Liu, and B. Zhang, "3D time-domain airborne electromagnetic inversion based on secondary field finite-volume method," *Geophysics*, vol. 83, no. 4, pp. E219–E228, Jul. 2018.
[58] H.-Y. Li, J.-X. Zhang, M.-Z. Jiang, Y. Luo, and D.-H. Sun, "The application effect analysis of VTEMplus system," *Geophys. Geochem. Explor.*, vol. 40, no. 2, pp. 360–364, Apr. 2017.
[59] D.-H. Sun, H.-Y. Li, M.-Z. Jiang, P.-J. Wang, Y. Luo, and Z.-F. Liu, "Applications of time domain airborne electromagnetic and aeromagnetic in Wulonggou gold deposit exploration area," *Progr. Geophys.*, vol. 32, no. 6, pp. 2533–2544, 2017.
[60] Y.-L. Ning, Z.-Y. Zhou, M.-Z. Jiang, Y. Luo, R.-H. Zhang, L. Zhu, and L.-H. Peng, "Airborne anomaly characteristics and prospecting intention of the upper reaches of Xiagalai'aoyi river Pb-Zn deposit in Heilongjiang," *Progr. Geophys.*, vol. 34, no. 3, pp. 1074–1080, 2019.
[61] Y.-Y. He, S.-J. Liang, and S. Lian, "Investigation of water distribution in Baoqing area using airborne transient electromagnetic technique," *Progr. Geophys.*, vol. 33, no. 5, pp. 2126–2133, 2018.
[62] M.-X. Yang and S.-J. Liang, "Analysis of influence factors on airborne electromagnetic survey in Fujin-Youyi area," *Sci. Technol. Eng.*, vol. 19, no. 3, pp. 48–54, Jan. 2019.

XIN WU received the Ph.D. degree in geophysics from the University of Chinese Academy of Sciences, in 2018. He is currently a Postdoctoral Researcher with the Key Laboratory of Mineral Resources, Chinese Academy of Sciences, with an emphasis in theory, technology, and application of the transient electromagnetic method.

GUOQIANG XUE is currently a Researcher with the CAS Key Laboratory of Mineral Resources, with an emphasis in grounded electric sources transient electromagnetic method. His researches focus on TEM pseudo-seismic interpretation methods, TEM tunnel predication studies, large loop TEM exploration technology, the TEM response of short-offset excited by grounded electric sources, and analysis of time-varying point charge infinitesimal assumptions in the TEM field.

YIMING HE was born in Liaoning, China, in 1995. He received the bachelor's degree in geophysics from the China University of Mining and Technology, in 2017. He is currently pursuing the Ph.D. degree with the Institute of Geology and Geophysics, Chinese Academy of Sciences. His main research direction is time domain electromagnetic prospecting, including the quasi 3-D inversion and denoise research.